Chiang Mai J. Sci. 2020; 47(1) : 114-126
http://epg.science.cmu.ac.th/ejournal/
Contributed Paper

Formulation and Physicochemical Properties of Nanostructured Lipid Carriers from Beeswax and Rosemary Oil as a Drug Carrier

Farhanim Mohd Latif, Yin Yin Teo*, Misni Misran, Vicit Rizal Eh Suk and Kah Hin Low

Department of Chemistry, University of Malaya, 50603 Kuala Lumpur, Malaysia.

*Author for correspondence; e-mail: yinyinteo@um.edu.my

Received: 17 June 2019
Revised: 23 August 2019
Accepted: 25 August 2019

Abstract

The toxicity and insolubility of drugs in water remain a significant problem and has led to the development of food-grade drug delivery systems such as nanostructured lipid carriers (NLCs). A stable colloidal suspension of NLCs was prepared from a natural source of lipids. NLCs composed of beeswax (BW), rosemary oil (RO), and poloxamer 188 (P188) were prepared using melt-emulsification combined with ultrasonication. The optimised formulation with the smallest particle size and highest magnitude of zeta potential was selected for loading with terbinafine hydrochloride (TBHCl). TBHCl is a synthetic allylamine drug that functions as an antifungal. The optimised formulation comprised 3.75 % BW, 1.25 % RO, 3 % P188, and 92 % deionised water (DW). The mean particle size and zeta potential of the optimised NLCs was 174 ± 2 nm and -36 ± 5 mV, respectively. The morphology of the NLCs was observed as spherical with a dense appearance in the TEM images. The encapsulation and loading efficiencies were found to be dependent on the amount of TBHCl. The release of TBHCl from the optimised formulation was 62.87 ± 0.04 % during the 48-hour analysis.

Keywords: colloidal; lipid; beeswax; rosemary oil; nanostructured lipid carriers

1. Introduction

NLCs is one type of lipid-nanoparticle that was firstly formulated at the end of the 1990s [1, 2]. It was evolved from solid lipid nanoparticle (SLNs) system. SLNs has a highly ordered crystalline structure due to the solid nature of lipid. As a consequence, there is restricted space remains in SLNs for drug incorporation. NLC could overcome the SLNs limitation by combining between solid lipid and liquid lipid/oil in it. This combination generates an imperfect matrix and less ordered arrangement of lipid matrix that enable incorporation and protection of the bioactive compounds efficiently. The solid lipid is the major component with the suggested amount in the range of 70 % to 90 % in NLCs [3]. NLCs have gained great attention as a promising drug control release system due to their functionality, biocompatibility, biodegradability, mass production, reduced risk of drug leakage, and long shelf-life. NLCs also assist in oral delivery of bioactive food components that can protect and improve their functionality [4].

The resulting NLCs help to improve the stability of the chemically-sensitive lipophilic ingredients.

In this context, the degradation rate of the active ingredients is slowed in the solid matrix as compared with the liquid matrix. The micro-phase separation between the active ingredients and carrier lipid, and within individual particles, can be managed to avoid the accumulation of active compounds at the surface of lipid particles where degradation used to take place. In addition, NLCs can maintain their solid state at room temperature by tuning the proportion of liquid lipid and hence aiding controlled release of the drug [5].

Many studies have investigated the preparation of NLCs using a variety of lipid materials, for instance, fatty acids, triglycerides, phospholipids, and waxes (that are found as solid lipids at both room and body temperature); however, only a limited number of these reports have involved food-grade lipids that are generally recognised as safe [6]. Good applicability of NLCs from edible sources has been demonstrated in the agricultural, food, and pharmaceutical industries. The use of natural remedies as food preservative in the preparation of NLCs will create an inexpensive, renewable system with high acceptability among consumers. Nowadays, the awareness among consumers regarding the connection between their nutritional habits and general health is increasing; hence, they are looking for foods containing multifunctional ingredients besides those that are necessary nutrients [4]. NLCs are also a potential encapsulation system in food science, which could be achieved using food-grade components. NLCs composed of food-grade drug and nutraceutical delivery formulations are a novel prospect of nanotechnology in nanodelivery science. The safety standard of food science is considered as important as pharmaceutical standards; however, it will have more serious consequences due to the long-term use of foods as compared with drugs. Drugs are taken occasionally, while foods are consumed regularly; hence, health and safety standards used in food science could certainly be practiced in pharmaceutical sciences.

There also exist a few studies related to wax-based NLCs. Wax-based NLCs are believed to become a more stable system and display good particle size distribution. Since there are no related reports regarding NLCs based on combination of BW and RO, therefore, this formulation was of interest. As a solid lipid, BW exists as simple esters with long hydrocarbon chains, the viscoelastic behaviour of which can be easily altered by the presence of free fatty acids; while the candidate RO possesses various pharmacological activities [7]. To disperse the lipids in aqueous solution, P188 was considered. Such non-ionic surfactants have shown great compatibility with most colloidal carriers in the formulation of pharmaceuticals, cosmetics, and food products [8]. The toxicity of P188 to humans and animals has also been investigated. No skin sensitisation data has been found from human testing [9]. In one reported study, P188 of dosages of (30, 100, 300, 720, 2400 or 72000) mg/kg/day were administered continuously to 20 male and female dogs via intravenous infusion for 30 days. Afterwards, plasma samples were taken during and after infusion. At the day 7, it remained a safe state for all the dose groups and P188 stable throughout the administration. Therefore, it displayed no effect of dose and gender of the P188 concentration on the plasma concentration [10].

The present study aimed to formulate food-grade NLCs using BW, RO, and P188 for the delivery of TBHC1. The drug carrier formulation was explored using response surface methodology for simultaneous optimisation of corresponding particle size and zeta potential. The particle size, polydispersity index, zeta potential, encapsulation efficiency, drug loading efficiency, and drug release of the TBHC1-loaded NLCs were characterised.

2. MATERIALS AND METHODS

All reagents used were of either pharmaceutical, food, analytical grade or better. Beeswax, cera alba (refined, yellow), rosemary oil, phosphate buffer saline (PBS) tablet, and TBHC1 were obtained from Sigma Aldrich, while poloxamer 188 from

Merck, and ethanol from R&M Chemicals. All solutions and samples were prepared by using deionized water with a resistivity of 18.2 MΩ cm at 25 ˚C.

2.1 Formulation of SLNs and NLCs

2.1.1 Melt-emulsification combined with ultrasonication method

Briefly, the mixture of lipids and surfactant was preheated at 75 ± 1 ˚C (which is higher than the melting point of the BW used), homogenised, and sonicated for 10 minutes using a sonic dismembrator (Model 505, Fisher Scientific, USA) at an amplitude of 50 %, and prior to being topped up with an appropriate amount of cold water to form an emulsion. From previous research, 10 minutes was sufficient to obtain small sized formulations [11]. Homogenisation and sonication for longer than 10 minutes would likely cause metal contamination from the probe, which would decrease the quality of the SLNs and NLCs [12]. There is not much difference between the preparation method for SLNs and NLCs; NLCs require solid and liquid lipids heated together with a surfactant, whereas SLNs need only solid lipid heated together with surfactant.

2.1.2 Design of experiments

The effects of the relative proportions of lipids, surfactant, and solvent on the particle size and zeta potential of the formulated lipid carriers were evaluated with an extreme vertices mixture design using JMP® 12 Statistical Discovery™ from SAS (USA). Table 1 shows the range of investigated variables and their linear constraints, and the randomised design matrix is illustrated in Table 2.

The responses obtained were modelled with Scheffe's quadratic polynomial as a function of the relative proportion of the components,:

$$y_i = \sum_i \beta_i X_i + \sum_{i,j} \beta_{ij} X_i X_j \qquad \text{(Equation 3)}$$

where β_i are linear coefficients, and β_{ij} are binary interaction coefficients of components i and j ($i \neq j$).

2.2 Long-term Stability Studies

A stability study was implemented to evaluate the effect of storage on the average particle size, polydispersity index, and zeta potential of the formulations. The measurement of these parameters was performed in triplicate. The formulations were stored in an airtight container and kept at room temperature (27 °C) for 84 days.

2.3 Encapsulation of TBHC1 in NLCs

TBHC1 was added to the mixture of BW and RO prior to heating and sonication to solubilise the drug and lipids, and hot P188 in deionised water at the same temperature (75 °C) was added to the mixture, which was subsequently homogenised and sonicated to form an emulsion using a sonic dismembrator. Cold water was then added to the emulsion to form NLC-encapsulated TBHC1.

Table 1. Ranges and constraints of the mixture proportions.

Control variable	Composition	
	Min	Max
Beeswax	0	0.1
Rosemary oil	0	0.05
Poloxamer 188	0.01	0.05
Deionized water	0	0.94
Linear constraints		
$0.05 \leq x_1 + x_2 \leq 0.1$	Equation 1	
$x_1 \geq x_2$	Equation 2	

Table 2. The designed matrix and responses.

Run/ Formulation	x_1	x_2	x_3	x_4	Mean particle size /nm	Mean zeta potential / mV
F1	0.05	0.05	0.05	0.85	163 ± 2	-32 ± 5
F2	0.05	0.05	0.01	0.89	727 ± 102	-38 ± 7
F3	0.075	0	0.05	0.875	144 ± 1	-34 ± 3
F4	0.0375	0.0375	0.03	0.895	217 ± 6	-38 ± 4
F5	0.05625	0.01875	0.01	0.915	585 ± 65	-39 ± 7
F6	0.05	0.05	0.03	0.87	265 ± 4	-38 ± 5
F7	0.075	0.025	0.05	0.85	188 ± 2	-38 ± 4
F8	0.1	0	0.01	0.89	836 ± 164	-39 ± 6
F9	0.05	0	0.05	0.9	140 ± 2	-34 ± 4
F10	0.075	0.025	0.03	0.87	269 ± 7	-39 ± 5
F11	0.05	0	0.01	0.94	448 ± 73	-41 ± 6
F12	0.025	0.025	0.05	0.9	133 ± 1	-33 ± 3
F13	0.1	0	0.05	0.85	168 ± 2	-35 ± 3
F14	0.05	0	0.03	0.92	163 ± 2	-37 ± 5
F15	0.0375	0.0375	0.05	0.875	155 ± 2	-34 ± 4
F16	0.0375	0.0125	0.03	0.92	174 ± 2	-36 ± 5
F17	0.0375	0.0125	0.01	0.94	418 ± 46	-39 ± 7
F18	0.05625	0.01875	0.05	0.875	161 ± 1	-34 ± 4
F19	0.05625	0.01875	0.03	0.895	219 ± 3	-38 ± 5
F20	0.0375	0.0125	0.05	0.9	122 ± 2	-30 ± 4
F21	0.025	0.025	0.03	0.92	184 ± 1	-42 ± 8
F22	0.1	0	0.03	0.87	216 ± 2	-38 ± 3
F23	0.075	0.025	0.01	0.89	532 ± 63	-37 ± 6
F24	0.075	0	0.03	0.895	215 ± 2	-39 ± 5
F25	0.075	0	0.01	0.915	597 ± 104	-39 ± 5
F26	0.0375	0.0375	0.01	0.915	632 ± 76	-42 ± 7
F27	0.025	0.025	0.01	0.94	452 ± 49	-43 ± 7

2.4 Physico-chemical Properties Characterization

2.4.1 Particle size and zeta potential measurement

Determination of particle size and zeta potential of SLNs and NLCs were conducted using a Malvern Nano series Zetasiser (Malvern Instrument, UK) at 25 °C with a backscattering angle of 173°. A sample volume of 0.5 mL was diluted in 25 mL deionised water prior to analysis. It is imperative to prepare a highly disperse system with minimum opacity in a sample; if the sample is too concentrated, the light scattered by one particle will be scattered by another particle or interpreted as multiple scattering. This condition produces a variable and inconsistent measurement. Three measurements were performed for each sample.

2.4.2 Field emission scanning electron microscopy (FESEM) and transmission electron microscopy (TEM)

The morphology of the NLCs was obtained

using a field emission scanning electron microscope (FESEM) (Hitachi, SU8220). A diluted NLCs sample was dropped onto a silicon slide and air dried prior to coating with platinum under vacuum conditions. The sample was subsequently examined.

The morphology of the NLCs also was viewed under a TEM (Carl Zeiss Libra®, 120). A drop of sample solution was placed onto a 400-mesh copper grid and left to adhere for 15 minutes. Excess sample solution was removed by blotting with filter paper, and the grid was then air dried and negatively stained with 1 % phosphotungstic acid. The sample was air-dried prior to visualisation under TEM. An acceleration voltage of 150 kV was applied.

2.5 Encapsulation and Drug Loading Efficiency

TBHC1 was encapsulated in the optimised formulation of NLCs. The ultrafiltration method was adapted to separate the non-encapsulated TBHCl from that encapsulated in NLCs. The concentrator body and filtrate vessel of Vivaspin® 6 was composed of polycarbonate, while the membrane was composed of polyethersulphone. The width and active membrane area of Vivaspin® 6 was 17 mm and 2.5 cm^2, respectively. Approximately 5 mL TBHC1 NLCs dispersion was placed in the upper chamber of centrifugal filter tubes with a 30 kDa cut-off (Vivaspin® 6, Sartorius stedim Biotech, Germany). Subsequently, the filled Vivaspin® 6 was centrifuged for 1 hour 30 minutes at 7000 rpm (5182 × g) to separate the non-encapsulated TBHC1 as the filtrate. NLCs encapsulated TBHCl remained in the upper chamber of the centrifugal filter tube. The supernatant in the lower part of the centrifugal tube was diluted to 5 mL with deionised water. The concentration of free drug in the supernatant was determined using a UV-Visible spectrophotometer (Cary®50) in a clear quartz cuvette, with a 1 cm path length, at a constant temperature of 25 °C. The concentration of drug in each sample was determined from the standard calibration curve (0.012 - 0.05 mg mL^{-1}) at wavelength of 284 nm.

Encapsulation efficiency and drug loading efficiency were calculated by using the equation (4) and (5), respectively:

$$\% \text{ EE} = [(C_T - C_F)/C_T] \times 100 \quad \text{(Equation 4)}$$

$$\% \text{ DL} = [(C_T - C_F)/C_L] \times 100 \quad \text{(Equation 5)}$$

C_T is the concentration of total drug in NLCs, C_F is the concentration of free drug in supernatant and C_L is the concentration of total lipid.

2.6 In vitro Drug Release Studies

In vitro drug release studies were performed using automated vertical clear-glass diffusion Franz diffusion cells (Hanson MicroettePlus™) with a 0.9 cm orifice diameter, 1 mL donor volume, and 4 mL receptor volume. A cellulose dialysis membrane with a 5 kDa cut-off was soaked in the receptor medium for at least 12 hours prior to mounting between the donor and receptor chambers. The donor chamber contained 1 mL sample dispersion, while the receptor chamber was filled with 1:1 (v/v) ethanol: PBS solution at pH 7.5, maintained at 37 °C with magnetic stirring at 400 rpm. At predetermined time intervals, the sample was automatically collected from the receptor chamber and replaced with the same volume of ethanol: PBS solution from the reservoir. The concentration of TBHC1 in the collected samples was determined using a Cary® 50 UV-Visible spectrophotometer with a 1 cm path length quartz cuvette, as compared with the standard calibration curve (0.002 - 0.008 mg mL^{-1}) at a wavelength of 284 nm. Replicates were conducted for each sample.

3. Results and Discussion

3.1 Mixture Design

3.1.1 Modelling of the mixture design response

Scheffe's quadratic models were postulated for particle size and zeta potential responses, with estimated regression coefficients as displayed in Table 3. The output from the analysis of variance

indicates that both the predictive models were statistically significant ($p < 0.0002$), with an R^2 of 0.96 and 0.80, and an RMSE of 54 and 1.7, respectively. Based on these results, the corresponding particle size and zeta potential were strongly dependent on the relative proportions of their ingredient, where significant second-order interactions were demonstrated between P188 and rest of the ingredients.

3.1.2 Effect of ratio of the mixture proportions

The effects of BW, RO, P188, and water content on particle size and zeta potential responses that predicted the centre point of the experimental region are presented in Figure 1. According to the predicted profile, the particle size of lipid carriers increased with increasing relative proportions of BW. This trend may be related to the overall increase in viscosity with increasing solid lipid content, which tends to reduce the effectiveness of homogenisation during production. Similarly, an increase in RO ratio increased the particle size, since the core of the carriers is loaded with more liquid oil. However, the reduction in particle size with increasing concentrations of P188 in the formulation may be related to the decreased interfacial tension between the lipid matrix and the aqueous phase [13, 14]. In view of the NLCs particle size was affected by mixture proportion, F16 produced the smallest particle size was selected in the preparation using PBS as a dispersed phase. The NLCs size in PBS was much smaller 144 ± 1 nm as compared with that in deionised water 174 ± 2 nm [15].

3.1.3 Optimization of the responses

For better visualisation of the effects, the predicted response domain fixed at 92 % water content is presented as a ternary contour plot (Figure 2). Considering the applied constraints (shaded domain), the simultaneous optimum responses for particle size and zeta potential were predicted to be 150 - 200 nm and 36 - 40 mV, respectively. From the result, it proved that 5 % of total lipid (3.75 % BW, 1.25 % RO) showed a smallest particle size and has presented a good stability (from zeta potential value). Hence, the formulation composed of 3.75 % BW, 1.25 % RO, and 3 % P188 was selected for further study.

3.2 Stability studies

The stability of NLCs can also be monitored via the measurement of particle size and zeta potential value during long-term storage of

Table 3. Estimated regression coefficients for particle size and zeta potential.

X	Particle size			Zeta potential		
	β	s_e	p	β	s_e	p
$x_1/0.19$	1013.819	499.1611	0.0582	-35.6658	16.04827	0.0401*
$x_2/0.19$	2069.566	1217.84	0.1075	1.244193	39.15415	0.975
$(x_3 - 0.01)/0.19$	10543	1640.077	<.0001*	141.3704	52.72928	0.0158*
$(x_4 - 0.8)/0.19$	112.5278	194.0146	0.5695	-41.7685	6.237663	<.0001*
$x_1 \bullet x_2$	-3049.99	1876.259	0.1224	-5.23603	60.32265	0.9318
$x_1 \bullet x_3$	-17375.8	2659.419	<.0001*	-259.697	85.5016	0.0074*
$x_2 \bullet x_3$	-17425.8	3151.682	<.0001*	-278.887	101.3281	0.0136*
$x_1 \bullet x_4$	576.7644	1314.241	0.6663	2.304943	42.25349	0.9571
$x_2 \bullet x_4$	-274.894	1881.928	0.8856	-74.147	60.5049	0.2371
$x_3 \bullet x_4$	-13823.3	1987.557	<.0001*	-145.403	63.90093	0.0361*

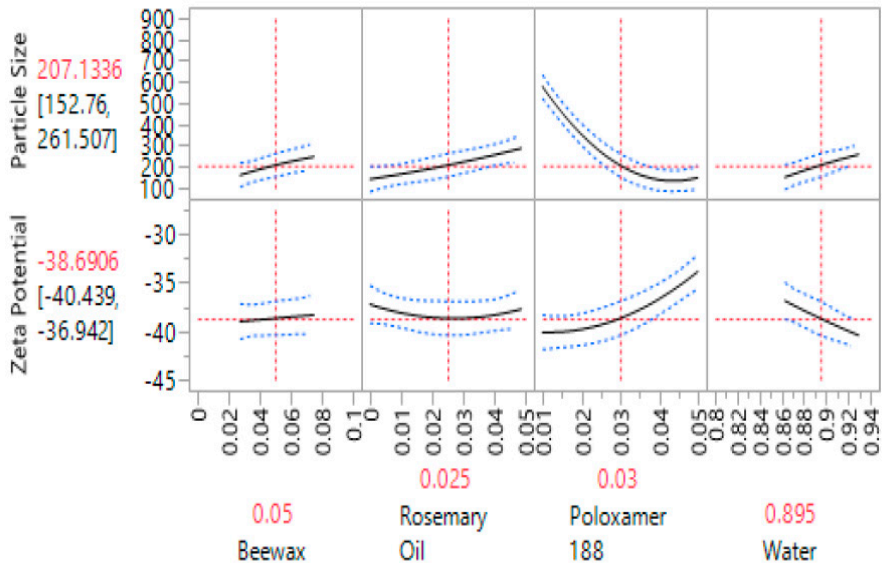

Figure 1. The predicted profiles showing the effect of each individual component.

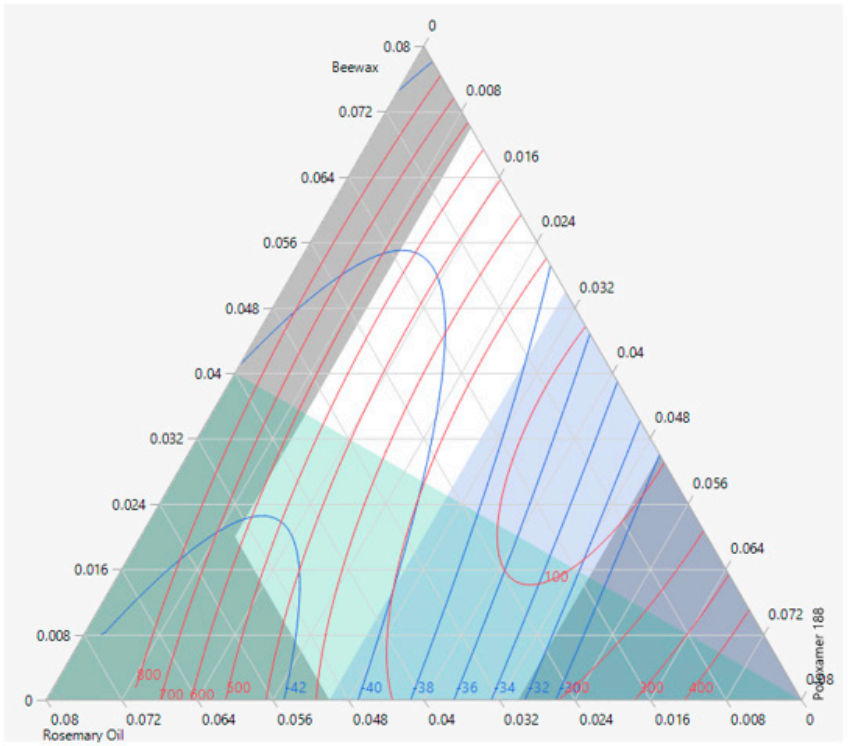

Figure 2. Ternary contour plot showing the effect of mixture on the particle size (red lines) and zeta potential (blue lines) of the formulated lipid carriers fixed at 92% water content.

formulations over 86 days. The presence of an appropriate amount of surfactant helps to stabilise the newly developed surfaces between the oil and water in the formulation, reducing the particle size [16]. In this case, the hydrophobic chains of P188 adsorb on the particle surfaces as the "anchor chain", while the hydrophilic chains extend out from the surface of the particle into the aqueous medium to create a stabiliser layer. However, the results suggest that 1% P188 was insufficient to prevent the aggregation induced by hydrophobic attraction, which may lead to instability and recrystallisation of the carriers. Figure 3 shows the fluctuating value of NLCs particle size and polydispersity index (PDI) over the 86-day analysis. A high PDI value indicates a very broad size distribution, while a small PDI value can be interpreted as a narrow size distribution. Moreover, the formulations with a high lipid concentration were observed to be physically less stable as compared with those with a low lipid concentration due to the greater size and recrystallisation ease. Furthermore, the zeta potential value can also predict stable formulations. As explained by previous research, a higher (close to 30 mV or higher) zeta potential value, whether negative or positive, is considered an indication of a stable dispersion. Based on Figure 4, the zeta potential values were depressed when the percentage of P188 was greater in the NLC formulations over the 86-day analysis, which is due to the adsorption of P188 onto the surface of the lipid nanoparticles. The probability of P188 adsorption onto NLCs is related to the percentage of P188 used in the formulations; increasing the P188 concentration promotes greater adsorption of P188 onto the NLCs. Therefore, NLCs with 1 % P188 have a more negative zeta potential value as compared with those with 3 % and 5 % P188. The adsorption of 1 % P188 onto the surface of lipid nanoparticles is weaker as compared with that of the 3 % and 5 % surfactant in the NLC formulations. Thus, 1 % P188 induced a higher zeta potential value due to the higher and effortless movement of particles that repelled each other on the slipping plane, which is the boundary at which the zeta potential was measured. For this reason, the compositional ratio must be finely adjusted

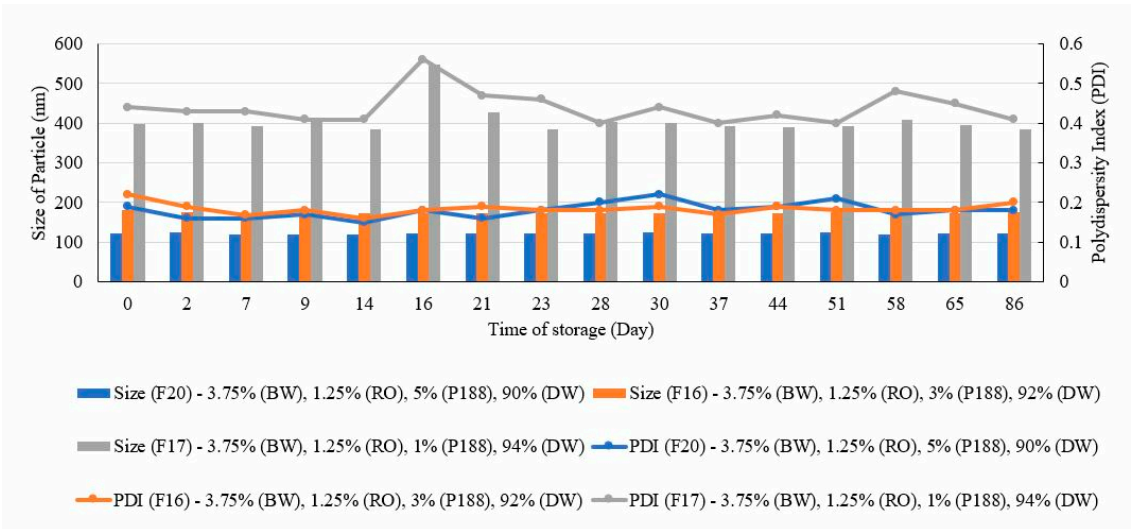

Figure 3. Size of particle and polydispersity index versus time of storage (day). The NLCs displayed were F17 (BW (3.75 %), RO (1.25 %), P188 (1 %) DW (94 %)), F16 (BW (3.75 %), RO (1.25 %), P188 (3 %) DW (92 %)) and F20 (BW (3.75 %), RO (1.25 %), P188 (5 %) DW (90 %)).

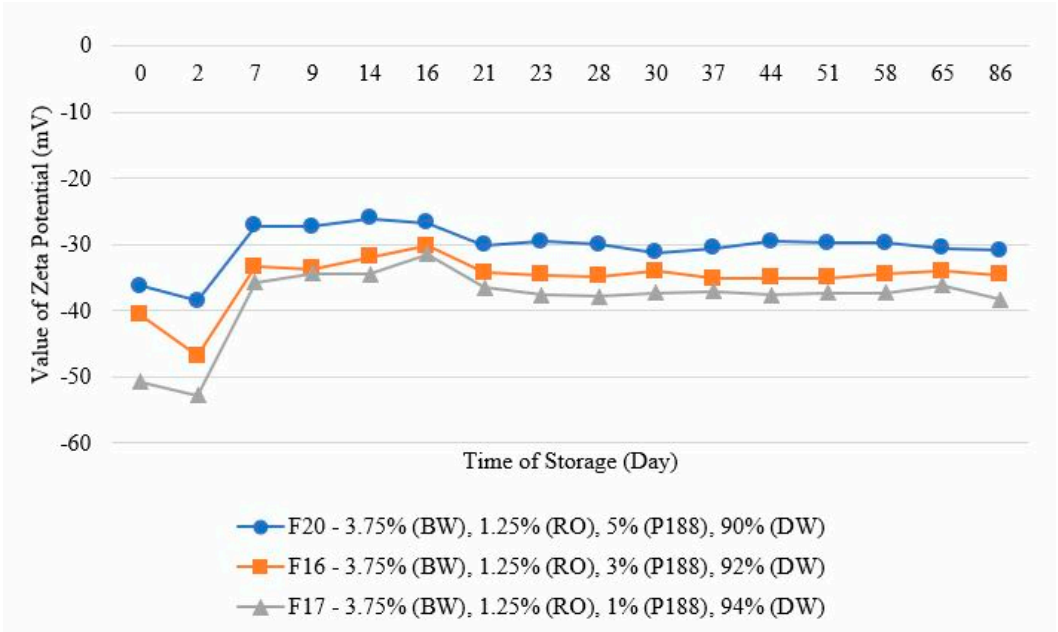

Figure 4. Value of zeta potential versus time of storage (day). The NLCs displayed were F17 (BW (3.75 %), RO (1.25 %), P188 (1 %) DW (94 %)), F16 (BW (3.75 %), RO (1.25 %), P188 (3 %) DW (92 %)) and F20 (BW (3.75 %), RO (1.25 %), P188 (5 %) DW (90 %)).

to produce NLCs with the desired particle size and stability. In addition, the zeta potential value for the F16 in PBS medium was reported as -18 ± 8 mV. The lower magnitude of zeta potential as compared with the NLCs in deionised water -36 ± 5 mV is possibly due to a charge-shielding effect in PBS [15].

3.3 Morphology of NLCs

Figure 5 (a) shows the TEM micrograph of the optimised NLC formulation, revealing a spherical shape with a dense appearance. NLCs were presented as individual non-aggregated particles. The particle size obtained from TEM was in agreement with that obtained from the zetasiser. The FESEM micrograph in Figure 5 (b) shows the presence of circular particles spread on the rough surface [4].

3.4 Drug Encapsulation and Drug Loading Efficiency of NLCs

The highest encapsulation efficiency of the optimised NLCs (F16) was found to be 99.50 ± 0.01 % at 0.04 mg mL^{-1}, as indicated in Figure 6. The encapsulation efficiency of TBHC1 in the optimised NLCs declined from 99.50 ± 0.01 % to 87.05 ± 0.05 % as the concentration of TBHC1 increased from 0.04 mg mL^{-1} to 0.5 mg mL^{-1}. On the other hand, the drug loading efficiency of TBHC1 in the NLCs increased from 0.29 ± 0.09 % to 3.20 ± 0.01 % as the concentration of TBHC1 increased from 0.04 mg mL^{-1} to 0.5 mg mL^{-1}, as revealed in Figure 6. More efficient drug loading into the NLCs occurred as the concentration of drug increased. The encapsulation efficiency of progesterone (drug) decreases as its concentration is increased. Inversely, the drug loading efficiency of progesterone increases as the drug concentration is increased [17]. Even though the encapsulation efficiency of the optimised NLCs was reduced with increasing concentration of drug, the drug loading efficiency was highly improved, indicating that the NLCs could be loaded with more drug. The arrangement of lipid in the NLCs

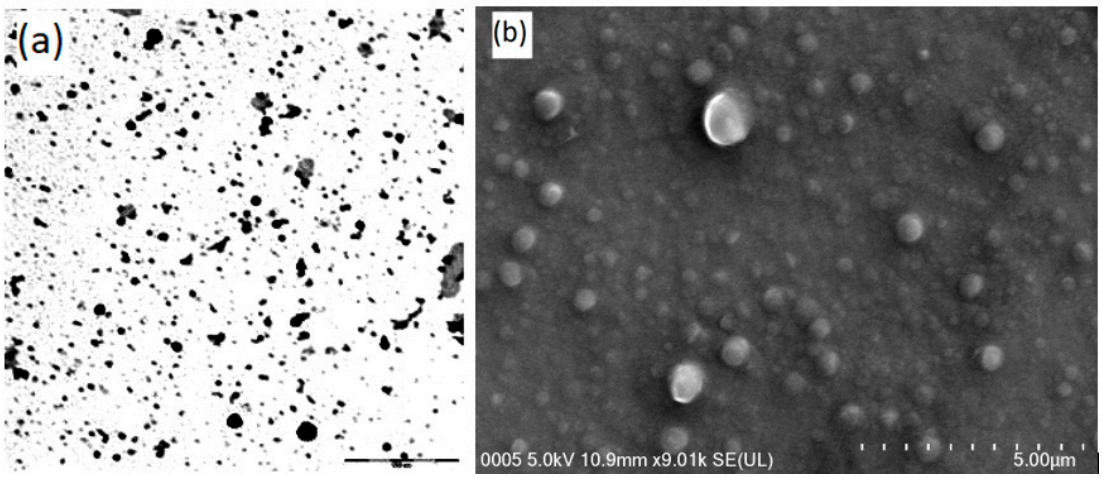

Figure 5. (a). Micrograph of NLCs (F16) through TEM (scale bar denotes size of 500 nm). **(b).** Micrograph of NLCs (F16) from FESEM.

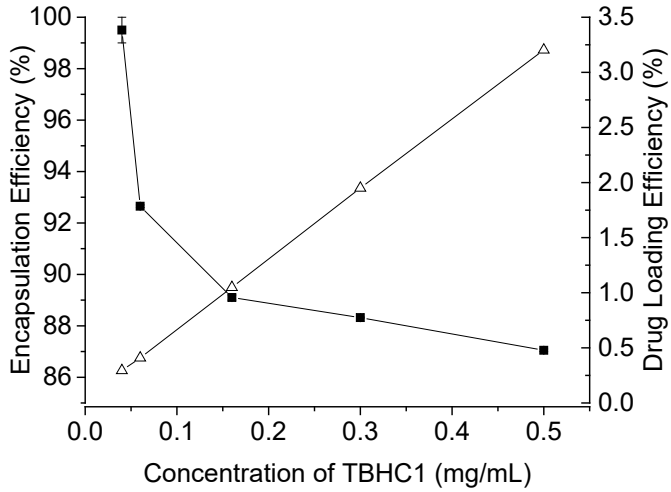

Figure 6. The effects of TBHC1 concentration on encapsulation efficiency (solid square) and drug loading efficiency (empty triangle).

became more imperfect, consequently providing sufficient space for a large amount of drug to be lodged effectively.

3.5 *In vitro* Drug Release Studies

Figure 7(a) shows the *in vitro* drug release of the NLCs (F16), SLNs (F14), and free drug solution over 48 hours. The concentration of TBHC1 in all samples was 0.1 mg mL^{-1}. This concentration was in the range of solubility for TBHC1 in deionised water [18]; thus, TBHC1 will be dispersed in the aqueous phase without forming any sediments on the bottom of the retentate. For the NLCs (F16), a biphasic drug release pattern was observed, indicating that TBHC1 was released quickly during the initial phase, followed by slow release from the NLC formulation. The initial rapid release may be due to diffusion of the free

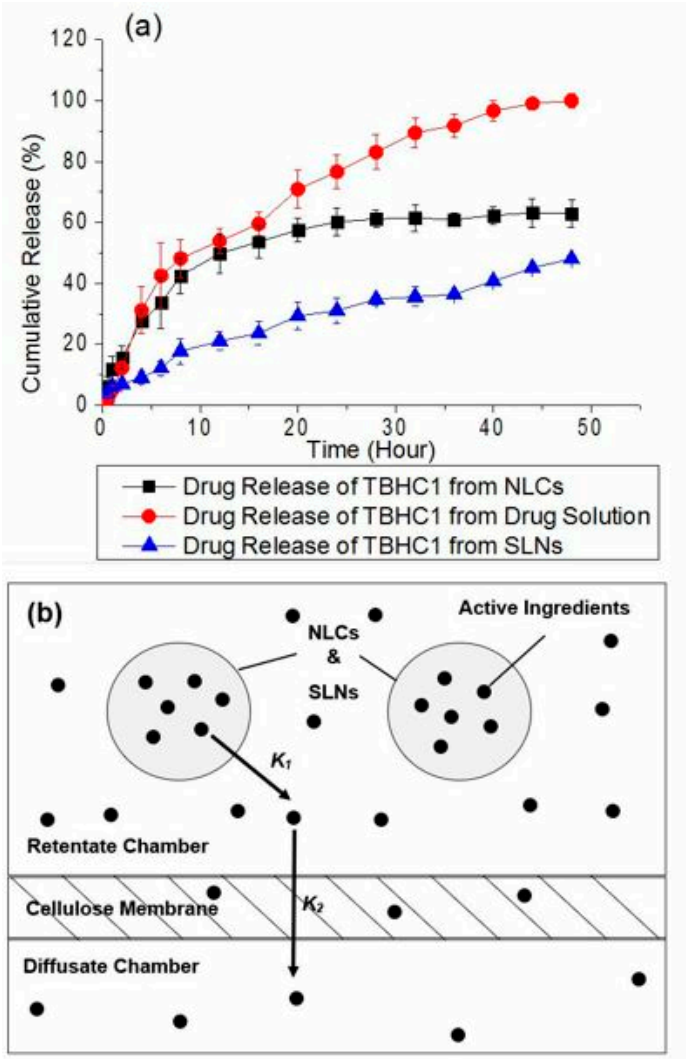

Figure 7. (a). Comparative in vitro release of TBHC1 in optimized NLCs (F16), SLNs (F14) and free drug solution. **(b).** Illustrated diagram for in vitro release mechanism of NLCs and SLNs with active ingredients in Franz diffusion cell.

drug from the aqueous phase (k_2). Subsequently, TBHC1 was released slowly and constantly from the NLCs and SLNs (k_1), as illustrated by Figure 7(b). The release of TBHC1 from the drug solution was faster 100 ± 0.07 % as compared with that from the optimised F16 NLCs, 62.87 ± 0.04 % and F14 SLNs, 48.07 ± 0.01 %. This may be due to the presence of lipid in the NLCs system, which can improve drug solubility and release potential. The presence of lipid in the system ensures sustained slow drug release from NLCs as compared with the free drug solution. Lipid also has the capability to produce a better release capacity by improving drug effectiveness and decreasing the side effects of the drug that are caused by rapid release from the free drug solution. The slow release of TBHC1 is due to the hydrophobic solid matrix of the NLCs and SLNs, which can retard the release of TBHC1 into the aqueous phase. The release of TBHC1

from the optimised F16 NLCs was higher 62.87 ± 0.04 % as compared with that from the F14 SLNs, 48.07 ± 0.01 %, indicating that drug release from the NLCs was increased by the addition of liquid lipid. This ensured that drug diffusion through the liquid lipid phase was faster as compared with that through the solid lipid phase, such as the SLN formulation. A similar observation was reported in a study by Uner and colleagues, in which it was found that loratadine (drug) was released slower from SLNs as compared with that from NLCs. The oil content of NLCs reduces the crystallinity and spontaneously facilitates faster drug-release as compared with SLNs [19].

4. Conclusion

In conclusion, NLCs were successfully prepared from beeswax, rosemary oil, and poloxamer 188 in the present work. F16 NLCs, consisting of 3.75 % BW, 1.25 % RO, 3 % P188, and 92 % deionized water, were chosen as the optimised formulation due to their physical stability for at least 86 days. The mean particle size and zeta potential of the optimised NLCs were found to be 174 ± 2 nm and -36 ± 5 mV, respectively. Moreover, NLCs promoted slow release of TBHCl as compared with the free drug solution, which may be due to the presence of lipid in the NLCs system, improving drug solubility and release potential. From the physicochemical characteristics, encapsulation efficiency, drug loading efficiency, and drug release, it can be suggested that NLCs are an excellent food-grade drug delivery system and could be a promising alternative vehicle for the delivery of various drugs to target tumor sites. This NLCs formulation can be tested in human and animal models in the future.

Acknowledgements

This research work was supported by University Malaya. It was financially supported by RU Grant – Programme Faculty (RF028B-2018), Prototype Research Grant Scheme (PR002-2018A) and Postgraduate Research Grant (PG075-2015B). The authors declare that they have no financial interest and conflict of interest.

References

[1] Doktorovova S., Souto E.B. and Silva A.M., *Eur. J. Pharm. Biopharm.*, 2014; **87**: 1-18. DOI 10.1016/j.ejpb.2014.02.005.

[2] Woo J.O., Misran M., Lee P.F. and Tan L.P., *Sci. World J.*, 2014; 1-7. DOI 10.1155/2014/205703.

[3] Wissing S., Kayser O. and Müller R., *Adv. Drug Deliver. Rev.*, 2004; **56**: 1257-1272. DOI 10.1016/j.addr.2003.12.002.

[4] Babazadeh A., Ghanbarzadeh B. and Hamishehkar H., *J. Funct. Food.*, 2016; **26**: 167-175. DOI 10.1016/j.jff.2016.07.017.

[5] Hu F.Q., Jiang S.P., Du Y.Z., Yuan H., Ye Y.Q. and Zeng S., *Colloid. Surface. B*, 2005; **45**: 167-173. DOI 10.1016/j.colsurfb.2005.08.005.

[6] Lasoń E., Sikora E. and Ogonowski J., *Acta Biochim. Pol.*, 2013; **60**: 773-777.

[7] Turasan H., Sahin S. and Sumnu G., *LWT - Food Sci. Technol.*, 2015; **64**: 112-119. DOI 10.1016/j.lwt.2015.05.036.

[8] Tamjidi F., Shahedi M., Varshosaz J. and Nasirpour A., *Innov. Food Sci. Emerg.,* 2013; **19**: 29-43. DOI 10.1016/j.ifset.2013.03.002.

[9] Singh-Joy S.D. and McLain V.C., *Int. J. Toxicol.*, 2007; **27**: 93-128. DOI 10.1080/10915810802244595.

[10] Grindel J.M., Jaworski T., Emanuele R.M. and Culbreth P., *Biopharm. Drug Dispos.*, 2002; **23**: 87-103. DOI 10.1002/bdd.297.

[11] Baek J.S., Pham C.V., Myung C.S. and Cho C.W., *Int. J. Pharmacol.*, 2015; **495**: 701-709. DOI 10.1016/j.ijpharm.2015.09.054.

[12] Liu C.H. and Wu C.T., *Colloid. Surface. A*, 2010; **353**: 149-156. DOI 10.1016/j.colsurfa.2009.11.006.

[13] Zirak M.B. and Pezeshki A., *Int. J. Curr. Microbiol. Appl. Sci.*, 2015; **4**: 924-932.

[14] Fathi H.A., Allam A., Elsabahy M., Fetih G. and El-Badry M., *Colloid. Surface. B*, 2018; **162**: 236-245. DOI 10.1016/j.colsurfb.2017.11.064.

[15] Bondì M.L., Azzolina A., Craparo E.F., Botto C., Amore E., Giammona G. and Cervello M., *J. Nanobiotechnol.*, 2014; **12**: 12-21. DOI 10.1186/1477-3155-12-21.

[16] Koroleva M.Y., Shcherbakov V.A., Khasanova L.K., Rakitin A.I., Shirokikh S.A. and Yurtov E.V., *Colloid J.+,* 2018; **80**: 272-281. DOI 10.1134/s1061933x18030079.

[17] Yuan H., Wang L.L., Du Y.Z., You J., Hu F.Q. and Zeng S., *Colloid. Surface. B*, 2007; **60**: 174-179. DOI 10.1016/j.colsurfb.2007.06.011.

[18] Debnath S., Kumar G.V. and Satayanarayana S., *Asian J. Pharm. Technol.*, 2013; **3**: 9-15.

[19] Üner M., Karaman E.F. and Aydoğmuş Z., *Trop. J. Pharm. Res.,* 2014; **13**: 663-680. DOI 10.4314/tjpr.v13i5.1.